The Astrophysical Journal, 588:387–399, 2003 May 1

GRB 021004: A MASSIVE PROGENITOR STAR SURROUNDED BY SHELLS

Bradley E. Schaefer, C. L. Gerardy, P. Höflich, A. Panaitescu, R. Quimby, J. Mader, G. J. Hill, P. Kumar, and J. C. Wheeler
Astronomy Department, University of Texas, Austin, TX 78712; schaefer@astro.as.utexas.edu, gerardy@astro.as.utexas.edu, pah@astro.as.utexas.edu, adp@astro.as.utexas.edu, quimby@astro.as.utexas.edu, jmader@astro.as.utexas.edu, hill@astro.as.utexas.edu, pk@astro.as.utexas.edu, wheel@astro.as.utexas.edu

M. Eracleous, S. Sigurdsson, P. Mészáros, and B. Zhang
Department of Astronomy, Pennsylvania State University, 525 Davey Lab, University Park, PA 16802; mce@astro.psu.edu, steinn@astro.psu.edu, nnp@astro.psu.edu, zhang@astro.psu.edu

L. Wang
Lawrence Berkeley Laboratory 50-232, 1 Cyclotron Road, Berkeley, CA 94720; lifan@panisse.lbl.gov

F. V. Hessman
Universitäts Sternwarte, Georg-August-Universität, Geismarlandstrasse 11, D-37083 Göttingen, Germany; hessman@uni-sw.gwdg.de

and

V. Petrosian
Center for Space Science and Astrophysics, Stanford University, 382 Via Pueblo Mall, Stanford, CA 94305; vahe@astronomy.stanford.edu
Received 2002 November 9; accepted 2003 January 10

ABSTRACT

We present spectra of the optical transient of GRB 021004 obtained with the Hobby-Eberly Telescope starting 15.48 hr, 20.31 hr, and 4.84 days after the γ-ray burst and a spectrum obtained with the H. J. Smith 2.7 m Telescope starting 14.31 hr after the γ-ray burst. GRB 021004 is the first burst afterglow for which the spectrum is dominated by absorption lines from high-ionization species with multiple velocity components separated by up to 3000 km s^{-1}. We argue that these absorption lines are likely to come from shells around a massive progenitor star. The high velocities and high ionizations arise from a combination of acceleration and flash ionization by the burst photons and the wind velocity and steady ionization by the progenitor. We also analyze the broadband spectrum and the light curve so as to distinguish the structure of gas within 0.3 pc of the burster. We delineate six components in the medium surrounding the γ-ray burst along the line of sight: (1) The $z \cong 2.293$ absorption lines arise from the innermost region closest to the burst, where the ionization will be highest and the 3000 km s^{-1} velocity comes from the intrinsic velocity of a massive star wind boosted by acceleration from the burst flux. For a mass-loss rate of $\sim 6 \times 10^{-5}\ M_{\odot}$ yr^{-1}, this component also provides the external medium with which the jet collides over radial distances 0.004–0.3 pc to create the afterglow light. (2) A second cloud or shell produces absorption lines with a relative velocity of 560 km s^{-1}. This component could be associated with the shell created by the fast massive star wind blowing a bubble in the preceding slow wind at a radial distance on the order of 10 pc or by a clump at $\sim$0.5 pc accelerated by the burst. (3) More distant clouds within the host galaxy that lie between 30 and 2500 pc and have been ionized by the burst will create the $z \cong 2.33$ absorption lines. (4–6) If the three bumps in the afterglow light curve at 0.14, 1.1, and 4.0 days are caused by clumps or shells in the massive star wind along the line of sight, then the radii and overdensities of these are 0.022, 0.063, and 0.12 pc and 50%, 10%, and 10%, respectively. The immediate progenitor of the γ-ray burst could be either a WC-type Wolf-Rayet star with a high-velocity wind or a highly evolved massive star the original mass of which was too small for it to become a WN-type Wolf-Rayet star. In summary, the highly ionized lines with high relative velocities most likely come from shells or clumps of material close to the progenitor, and these shells were plausibly produced by a massive star soon before its collapse.

Subject headings: gamma rays: bursts — stars: Wolf-Rayet

1. INTRODUCTION

The large absorption line redshift measurements settled the issue that most γ-ray bursts are at cosmological distances. The physical mechanism of the origin of the γ-ray bursts, questions of whether there are more than one mechanism, and the issue of whether γ-ray bursts interact only with the interstellar medium (ISM) or with a circumstellar environment are still very open. Correlations with star formation and observations of putative iron lines with the *Chandra X-Ray Observatory* (Piro et al. 2000) have put new focus on the connection to a supernova-like core collapse event.

Currently, most observations of γ-ray burst afterglows are photometric, with the effort being to find the power-law behavior of the afterglow brightness as a function of wavelength and time. Most of the 25 known redshifts have been measured by deep spectroscopy on the host galaxy long after the afterglow has faded. Prior to GRB 021004, only eight γ-ray burst afterglows have had early-time spectra that reveal absorption lines from the host galaxy (e.g., Vreeswijk et al. 2001). Of these, virtually all have been low-excitation

lines in one velocity system that are likely to arise in gas far from the burster. Two exceptions to this are GRB 011211, which shows C IV and Si IV in addition to lower excitation lines (Holland et al. 2002a), and GRB 010222, which displayed two low-ionization systems separated by $\sim$119 km s^{-1} that could arise from clouds at different positions within the host galaxy (Mirabal et al. 2002b). GRB 020813 has a spectrum that displays C IV absorption lines in both $z = 1.223$ and $z = 1.255$ systems (Barth et al. 2002). With so little known, and many afterglows revealing new properties, more prompt spectroscopy is clearly needed.

Afterglow spectra could show absorption lines arising from the host galaxy (especially the Fe and Mg ISM lines) that will give the redshift. The redshift is the key parameter for determining the burst energetics and hence further testing the conclusions of Frail et al. (2001) and Panaitescu & Kumar (2001) that γ-ray bursts have a nearly constant total energy. One can also improve the calibration (currently based on nine events; see also Schaefer, Deng, & Band 2001) that the spectral lags and light-curve variability are Cepheid-like luminosity indicators that could turn γ-ray bursts into a premier tool for cosmology out to $z \sim 10$ (Schaefer 2003). Intrinsic afterglow spectral features of any kind would be a boon to interpretation. If there are underlying supernova-like explosions, corresponding spectral features could be superposed on the continuum and revealed by careful subtraction of the well-defined power-law continuum. Detection of, for instance, features of redshifted Ca H and K lines, which tend to be among the strongest lines in all types of supernovae, would yield both a redshift and clues to the nature of the explosion itself. Other possibilities would be to discover Fe emission lines, which would yield temperatures, redshifts, and abundances. Perhaps the most important possibility is that of serendipitous discovery of some unexpected feature.

GRB 021004 provided an unprecedented opportunity to obtain prompt spectroscopy of the early afterglow of a γ-ray burst. GRB 021004 was discovered by instruments on the *High Energy Transient Explorer 2* (*HETE-2*) satellite at 12:06 UT on 2002 October 4 (Shirasaki et al. 2002). Prompt discovery of the optical transient by Fox et al. (2002a) allowed rapid spectroscopic observations. Fox et al. (2002b) obtained the first spectra and identified two intervening systems at $z = 1.38$ and 1.60 from Mg I and Mg II absorption, respectively. Eracleous et al. (2002) confirmed those features, noted several Fe II absorptions at these redshifts, and pointed out four absorption lines at $\sim$4633, 4664, 5109, and 5152 Å (see also Sahu et al. 2002; Castander et al. 2002). These were identified by Chornock & Filippenko (2002) as C IV and Si IV features at redshift of $\sim$2.3. Chornock & Filippenko also identified Lyα emission at $z = 2.323$ and absorption components and perhaps Lyβ at similar redshifts. Salamanca et al. (2002) identified four absorption components of C IV at $z = 2.295$, 2.298, 2.230, and 2.237, noting that the total spread is about 3000 km s^{-1}. They remarked that this velocity dispersion would be difficult to interpret as due to a single cluster of galaxies and noted that if associated with a supernova shell the supernova must have substantially preceded the γ-ray burst to be optically thin. Mirabal et al. (2002a) suggested the identification of one absorption feature as low-excitation Al II at $z = 2.328$ and identified that, and the Lyα emission, as the redshift of the host galaxy. They raised the issue of the velocity dispersion being due to a wind in a Wolf-Rayet–like progenitor. Djorgovski et al. (2002) noted that the Lyα flux may imply a strong star formation rate in the host galaxy. Savaglio et al. (2002) reported a very high resolution spectrum ($R = 50,000$) that revealed the complex fine structure of many of the high-ionization lines. They determined that the individual C IV features show complex flow spanning about 1000 km s^{-1} and conclude that the $z \cong 2.326$ system is probably close to the γ-ray burst. They note that of the four high-redshift systems, the low-ionization lines, Al II and possibly Si II, only occur in the highest redshift, $z \cong 2.326$, component. Matheson et al. (2003) and Møller et al. (2002) have provided an excellent compendium of line identifications along with detailed line profiles. Matheson et al. (2003) give a spectral index in the optical of $F_\nu \propto \nu^{0.96\pm0.03}$ and report a reddening of the continuum in the blue region of the spectrum over the first 3 days.

Here we report spectra obtained within the first day after outburst and 5 days later. We concentrate on constraining the circumburst medium in the context of the high-ionization lines and the afterglow light curve.

2. OBSERVATIONS

Spectra of the optical afterglow were obtained with both the 2.7 m Harlan J. Smith Telescope using the IGI imaging spectrograph (Hill et al. 2003) and the 9.2 m Hobby-Eberly Telescope (HET) with the Marcario Low-Resolution Spectrograph (Hill et al. 1998) at McDonald Observatory. Three consecutive exposures of 900 s each were taken with the 2.7 m telescope beginning 14.31 hr after onset of the γ-ray burst, followed by sets of three 900 s exposures taken with the HET beginning at 15.48 hr, 20.31 hr, and 4.84 days after the burst. A 2.″5 slit was used for the 2.7 m data, while the HET observations utilized a 2.″0 slit, giving all data sets a 16 Å resolution. The spectra were reduced using IRAF[1] and wavelength calibrated using argon, neon, cadmium, and mercury lamps. The combined spectrum from the first night is displayed in Figure 1.

Our first night spectrum shows a collection of absorption lines longward of 5800 Å that arise from iron and magnesium of relatively low ionization at redshifts of 1.38 and 1.60. These are due to intervening galaxies with no relevance to the γ-ray burst analysis. The lines at redshifts of $z \sim 2.3$ are presented with their measured properties in Table 1. The lines are separated into two primary velocity components, with $z \cong 2.326 \pm 0.001$ and $z \cong 2.293 \pm 0.003$. We identify the 4587.2 Å line as being from Si IV (cf. Matheson et al. 2003). There are few resonance lines from the ground state of highly ionized elements of high cosmic abundance in the observed wavelength range, and the only one that has not produced a detected absorption line is N V with rest wavelengths 1238.8 and 1242.8 Å for which we can only present an upper limit to its equivalent width.

The separation of the two high-redshift primary velocity components corresponds to a relative velocity of 3000 km s^{-1} in the frame of the host galaxy. The unblended lines for the $z \cong 2.326$ velocity component are significantly resolved in our spectrum, with an FWHM of $\sim$1000 km s^{-1}. From our own data, this implies either multiple components or

[1] IRAF is distributed by the National Optical Astronomy Observatory, which is operated by the Association for Research in Astronomy, Inc., under cooperative agreement with the National Science Foundation.

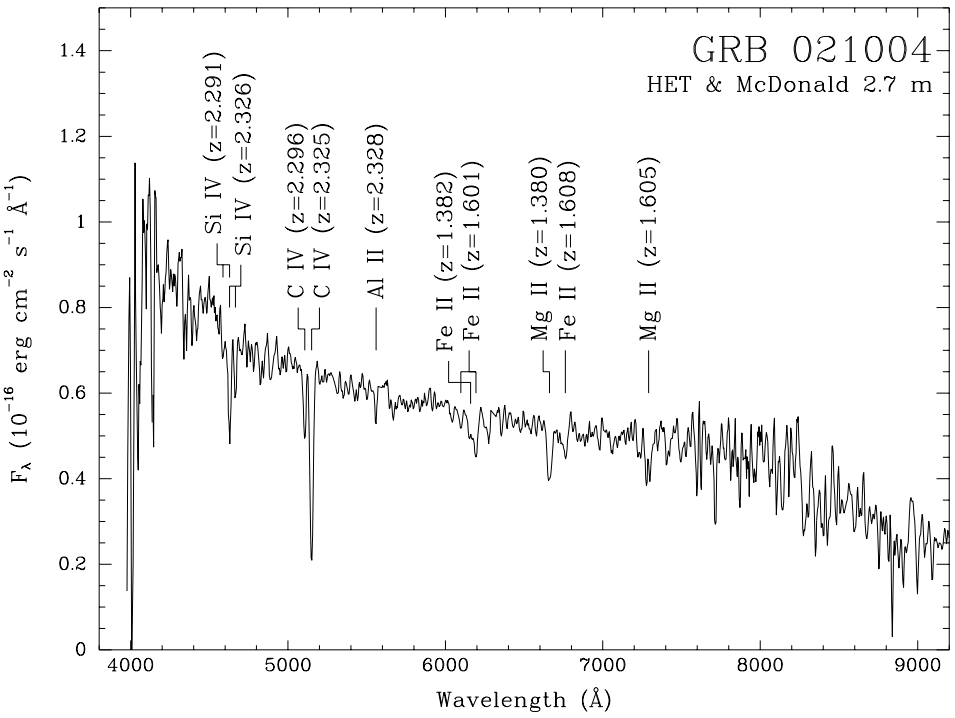

FIG. 1.—Combined spectrum for the first night. The absorption lines longward of 5800 Å are due to intervening galaxies at redshifts of 1.38 and 1.60. The primary lines of interest are the C IV lines from 5106 to 5150 Å and the Si IV doublet from 4587 to 4666 Å. Key points in our analysis are that these are highly ionized lines and that there are multiple velocity components that span a velocity of 3000 km s^{-1}. We identify the lines with redshift of around 2.293 as coming from a shell around the progenitor at a distance of less than a parsec.

one component with a velocity range that large. Other spectra (Savaglio et al. 2002; Mirabal et al. 2002a; Salamanca et al. 2002; Møller et al. 2002) have resolved the high-redshift component into at least two subcomponents with a velocity separation of 560 km s^{-1}. Thus, the $z \sim 2.3$ system consists of at least three separate velocity components, with velocities of 0, 560, and 3000 km s^{-1} toward Earth relative to the highest redshift component.

Draine & Hao (2002) presented detailed calculations of the complex of absorption lines produced from 1110 to 1705 Å by vibrationally excited molecular hydrogen in a molecular cloud near a γ-ray burst. Individual lines have a typical depth of 20% for normal low-resolution spectra and might be difficult to detect without very high signal. Fortunately, the entire pattern of lines is characteristic of the process, and so all of the lines (with their unique positions and depths) can be simultaneously sought in any spectrum. The idea is that a spectrum in which any one line would be highly insignificant might yet have the presence of many lines detectable at a high confidence level. Even a noisy spectrum might have its apparent noise following the characteristic molecular hydrogen features, thus resulting in a significant detection. Many of the individual lines are extremely saturated with optical depths of greater than 300 in the line center and with equivalent widths of 0.1 Å or greater, so that the strength of the absorption is quite insensitive to the column density of vibrationally excited molecular hydrogen, $N(H_2^*)$. B. Draine (2002, private communication) has

TABLE 1
LINE LIST FOR $z \sim 2.3$ COMPONENT

Line Identification	λ_{obs} (Å)	λ_{rest} (Å)	$EW_{obs}/(1+z)$[a] (Å)	z[b]
Si IV	4587.2 ± 3.6	1393.8	0.60 ± 0.24	2.291
Si IV[c]	4628.8 ± 1.3	1393.8	2.44 ± 0.30	2.321
Si IV[c]	4628.8 ± 1.3	1402.8	2.44 ± 0.30	2.299
Si IV	4665.9 ± 1.8	1402.8	1.17 ± 0.24	2.326
C IV	5106.2 ± 0.9	1548.2 and 1550.8	1.39 ± 0.12	2.296
C IV	5149.9 ± 0.4	1548.2 and 1550.8	5.42 ± 0.18	2.325
Al II	5559.9 ± 3.5	1670.8	0.66 ± 0.33[d]	2.328
N V	~4095	1238.8 & 1242.8	≤ 0.30	~2.3

[a] The observed equivalent width measured in angstroms corrected to the rest frame of the burst.
[b] The uncertainty in redshift z is 0.001–0.002.
[c] The 4628.8 Å line is a blend of the two Si IV doublet lines from the two redshift components.
[d] This line is close to the bright night sky line at 5575 Å, so there might be significant systematic uncertainties in the equivalent width due to imperfect night sky subtraction.

kindly provided us with the transmission spectrum for excited molecular hydrogen for our spectral resolution. We have used this as a template to cross-correlate with our spectrum. For a redshift of 2.3, we cover the range from 1240 to 1705 Å. We find no significant correlation peak for any redshift of the template. Within the redshift range of 2.29–2.33, the largest peak in the cross-correlation is never more than the rms of the cross-correlation over a much wider redshift range. The implication of this negative result will be discussed in § 3.5.

We found no significant differences among our spectra within the first night. Specifically, the equivalent widths of the absorption lines were all identical to within the errors. We have constructed broadband photometry from our reduced spectra using the photometric passbands of Landolt (1992) and normalizing the colors to match the observations concurrent to the 2.7 m spectrum. The resulting synthetic photometry for the B, V, and R magnitudes yields colors that are constant to within 0.04 mag for the first night.

For a comparison between our observations on the first and fifth nights, we are handicapped by the poor signal on the fifth night because of the faintness of the afterglow. The only lines for which we can quote line widths on the fifth night are the two C IV lines, which have equivalent widths in the rest frame of the host (the observed width divided by $1 + z$) of 1.0 ± 1.6 and 5.7 ± 2.4 Å at the same wavelengths as for the first night. This is consistent with the first night. We confirm the report by Matheson et al. (2003) that the blue end of the continuum became redder from the first night to subsequent nights. In particular, our synthetic photometry shows the $B-V$ color to have reddened by 0.25 ± 0.13 mag from the first to the fifth night, while the $V-R$ color was unchanged, 0.01 ± 0.07 mag, over the same interval.

3. THE HIGH-IONIZATION FEATURES

3.1. *The Source of the Absorbing Gas*

The Lyα *emission* line is likely to represent the average velocity of the host galaxy, although its exact wavelength will shift redward somewhat because of the absorption component. The redshift of the Lyα line is variously given as 2.3351, 2.332, 2.328, and 2.323 (Møller et al. 2002; Matheson et al. 2003; Mirabal et al. 2002a; Chornock & Filippenko 2002). The average velocity of the host galaxy is also likely represented by the low-ionization feature of Al II at 2.328. The highest redshift components of the C IV and Si IV lines correspond to this host galaxy velocity. The velocity of the burster itself might vary by up to several hundred km s^{-1} from the average velocity for the host. The other primary components of these high-ionization lines are at velocities of 560 and 3000 km s^{-1} blueward of the host galaxy velocity.

The presence of the $z \sim 2.3$ lines of C IV and Si IV shows that the absorbing gas is highly ionized. Such lines are commonly seen in the spectra of distant quasars through intervening galaxies where the ionized material is in a collisionally ionized halo. Could the absorbing gas for GRB 021004 just be in halos of chance galaxies along the line of sight? The presence of three velocity components within the $z \sim 2.3$ system with separation of up to 3000 km s^{-1} argues strongly that this cannot be. The probability of two galaxies lying in so small a redshift range just blueward of the host is rather small even in a cluster of galaxies, and the velocities are too large to allow for a bound cluster. Sargent, Steidel, & Boksenberg (1988) present statistics on lines with rest-frame equivalent widths of more than 0.3 Å (i.e., a threshold much smaller than the observed lines for GRB 021004) and find that absorption systems with $z \sim 2.3$ occur with a rate of $\sim$1.5 per redshift unit. The probability of getting two absorbers within a range of 0.033 in z in front of the host galaxy is thus 0.0024. Such an occurrence is not impossible (see the $z \sim 2.85$ system for Q1511+091; Sargent et al. 1988), but it is too small to be plausible for GRB 021004. It is also improbable that random intervening galaxies will have equivalent widths as thick as 1.4 Å (as for the observed C IV lines from the systems blueward of the host galaxy). The distribution of equivalent widths (for both members of the C IV doublet) falls off exponentially such that the probability for any one galaxy being above this threshold is $\sim$0.2, or 4% for both systems. In all, the probability of getting two chance galaxies with a redshift within 0.033 of the host and with rest-frame equivalent widths of $\geq$1.4 Å is 0.00010. We conclude that the high-ionization absorption lines are not from intervening galaxies.

The only other situation for which the C IV and Si IV lines are seen in absorption is when gas is subjected to a high flux of ionizing radiation, as in an active galactic nucleus (AGN), a Wolf-Rayet star, or a γ-ray burst. An AGN at the position of the γ-ray burst would already have been detected, and so this possibility can be rejected. With only $\sim$3100 Wolf-Rayet stars in our own Galaxy, the odds of the line of sight passing close to one to three such stars is small (ignoring clustering) provided that the star is not the progenitor of the γ-ray burst. That the progenitor is itself a Wolf-Rayet star is plausible, because the progenitor is likely to be a massive star just before a core collapse. Alternatively, the ionizing radiation could come from the γ-ray burst itself. Thus, we think that the most likely means to ionize the gas to high levels is either radiation from the burst progenitor or the burst itself, with both cases requiring the ionized gas to be physically associated with the burster.

3.2. *Ionizing the Gas*

Wolf-Rayet stars have temperatures from 30,000 to 70,000 K and supergiant luminosities. For the hotter stars, this is sufficient to ionize the surrounding nebulosity to levels where a significant fraction of the carbon and silicon atoms can produce C IV and Si IV absorption and emission. Thus, a Wolf-Rayet–like progenitor might already ionize the surrounding gas such that later light from the afterglow will have silhouettes of these high-excitation lines.

Alternatively, the γ-ray burst itself is an obvious source of a huge ionizing flux. The most frequent mode of ionization of carbon and silicon will be for the γ-ray to knock out an inner electron, whereupon autoionization will cause ejection of the valence electrons. In addition, the ejected electrons will have sufficient energy to ionize other atoms. In the remainder of this section, we will estimate a crude distance range over which the burst flux can ionize enough gas so as to produce the observed absorption lines.

The cross section for photoelectric interactions varies strongly with photon energy, so the probability that any given atom is ionized by burst flux requires an integral over energy. The cross sections for carbon and silicon are

tabulated in Höflich, Khokhlov, & Müller (1992) along with a prescription for interpolation. For carbon, the cross sections are 0.0213, 40.3, and 44500 barns (1 barn equals 10^{-24} cm^2) at photon energies of 100, 10, and 1 keV, respectively. With this, we see that most of the ionization will be from burst photons in the X-ray band.

The burst spectrum has only been measured down to a photon energy of 7 keV (23 keV in the frame of the host galaxy) by *HETE-2*. Above 7 keV, Lamb et al. (2002) state that the spectrum is well fitted by a single power law such that $dN/dE \propto E^{-1.64}$ and has a fluence from 7 to 400 keV of 3.2×10^{-6} ergs cm^{-2}. Below 7 keV, the spectrum will likely turn over to asymptote at a slope close to the synchrotron limit of $dN/dE \propto E^{-2/3}$. Here we will model this behavior as a broken power law with indices of -1.64 and -0.66 above and below a break energy, $E_{\rm break}$. We also impose a lower energy cutoff in our calculations at $E_{\rm cutoff}$, below which we assume that no flux reaches the gas. This is to model the possible photoelectric absorption of photons before they reach the gas. We normalize this spectrum to the 7–400 keV fluence reported by *HETE-2* and correct the photon energies of this observed spectrum by a factor of $1 + z$ to get the spectrum as seen by gas in the host galaxy frame.

The expectation value for the number of times that a given atom will be ionized by burst flux is $\int\int (dN/dE)\sigma\, dt\, dE$, where dN/dE is the burst photon spectrum (in units of photons cm^{-2} s^{-1} keV^{-1}) as a function of distance from the burster, σ is the cross section for ionization as a function of photon energy E, and t is the time. For these calculations, we adopt $E_{\rm break} = 7$ keV. We find that the result is highly sensitive to the value of $E_{\rm cutoff}$ (owing to the large cross section for ionization at low energies), which itself is highly uncertain since we do not know the degree of absorption of the low-energy photons before the radiation hits the gas. For $E_{\rm cutoff} = 0.3$ keV in our rest frame (1 keV in the host galaxy), we expect $\sim$100 ionizing interactions per carbon atom at a distance of 1 pc. For $E_{\rm cutoff} = 0.03$ keV in our rest frame (0.1 keV in the host galaxy), we expect $\sim$600 ionizing interactions per carbon atom at a distance of 1 pc. The expected number of ionizing interactions will scale as the inverse square of the distance. For this range of cases, the expected number of ionization interactions is unity at distances ranging from 10 to 25 pc. This provides an order-of-magnitude estimate of the minimal range out to which the burst flux will completely ionize carbon.

The radius at which significant high-ionization absorption can be caused may be substantially farther than this calculated distance for two reasons. First, only a small fraction of the carbon need be ionized to result in significant absorption. Since the cross section for the C IV resonance line is large, the intervening gas need only have a column density of 10^{14} cm^{-2} in the C IV state to account for the observed absorption line. This corresponds to a fraction of $\sim$0.0003 of the total carbon expected in a smooth wind (see § 3.4). If only 0.01% of the carbon must be ionized to C IV to create the necessary column density, then the burst's effective radius for ionization is larger than the previous distance estimate by a factor of 100. This factor depends on the column density of the cloudy ISM. Second, the electrons ejected from the neutral atoms at high velocity will also have a high cross section for ionizing further atoms. This effect depends on the density of the gas and the spectrum of the electrons (Lotz 1967). This effect will roughly increase the ionizing radius by a factor of the square root of the ratio of the electron energy to the ionization energy, which might be up to a factor on the order of 10. In all, there are many uncertainties and dependencies on unknown conditions, but the effective ionization radius of the burster might be on the order of 10–100 times larger than calculated in the previous paragraph. This would imply that any gas cloud within perhaps 100–2500 pc of the burster will suffer enough ionization to create a sufficient column density of C IV so as to form a detectable absorption line.

The complementary question is how close to the burster some gas will be incompletely ionized at the epoch of observation. This is important since we later consider the possibility of the absorbing gas being quite close ($\sim$0.2 pc) to the burst. Lazzati & Perna (2002) have presented a detailed and extensive calculation that shows that even a very thick wind will have all of its gas completely ionized by a GRB flash on timescales of milliseconds or faster. The implication is that most (if not all) of the atoms of carbon in a wind will also be completely ionized, and thus there may be no atoms in the C IV state to create absorption lines near the burst.

Whereas Lazzati & Perna considered a smooth wind, the column density of C IV $\sim 10^{14}$ cm^{-2} could be accounted for by clumps in the gas. The existence of such clumps is plausible since images of Wolf-Rayet winds show structure on all size scales. Also, the quasi-stationary flocculi (clumps of gas created in the Wolf-Rayet progenitor wind) in Cas A and the Kepler supernova remnants have densities of $(1\text{–}2) \times 10^4$ cm^{-3} (Gerardy & Fesen 2001) after correcting by a factor of 4 for the shock jump conditions, with a typical projected size of 5×10^{16} cm in width and 15×10^{16} cm in length. For GRB 021004 in particular, the existence of clumps is indicated by the three bumps in the afterglow light curve (see § 5) where the clumps might be large in size with moderate contrast or might be small in size yet with large central densities. The existence of clumps in the winds of massive stars is thus expected, and these clumps can have densities $\gtrsim 10^4$ cm^{-3}.

Clumps can serve in two ways to allow for the existence of C IV close to the γ-ray burst. First, the clump will shield portions of the wind material (both within the clump and within the shadow of the clump) from the high burst flux. For example, a clump with size 10^{17} cm with a density of 10^4 cm^{-3} at a distance of a fraction of a parsec from the burster should absorb the ionizing flux. Second, the higher density within clumps can allow for faster recombination that can generate C IV a day after the burst even if the burst had completely ionized the carbon. The degree of recombination that will have occurred when we see the absorption a day or so after the burst has ionized the gas depends strongly on the density. For ionized carbon, the recombination timescale is $\sim 10^5$ days for densities of 10 cm^{-3} that would be typical of a Wolf-Rayet wind at a distance of $\sim$0.1 pc. The recombination timescale would be $\sim$100 days for densities of 10^4 cm^{-3} that are typical of the densities observed in supernova remnant knots that are presumed to have formed in the progenitor's wind. Within such clumps, the fraction of carbon in the C IV state should be $\sim$0.01 a day after the burst. A clump with density 10^4 cm^{-3} and size 10^{17} cm will produce a column of 10^{19} cm^{-2} in C IV. This is 10^5 times larger column than is required to produce the observed absorption lines. Detailed calculations of the ionization structure are difficult without knowledge of the density structure in the wind. Nevertheless, it appears that shadows

and recombination in the expected clumps can yield a C IV column density of 10^{14} cm^{-2} even quite close to the burster.

The calculation of the ionization structure is not straightforward even if the density structure is given. One trouble is that the burst spectrum below 7 keV is unknown, and this is the critical energy region for ionizing the gas due to the large cross sections for photoionization. A related problem is accounting for the ionizing flux from the afterglow, which is comparable to that from the burst itself. An additional problem is that stimulated recombination will ensure that some fraction of the carbon will not be completely ionized even in a radiation field of the highest intensity. Yet another issue is that the photoionized electrons likely have roughly a power-law energy distribution, whereas the cross sections for ordinary and stimulated recombination are calculated for thermal electron distributions. The correct recombination rates are likely to be significantly different from the "usual" calculations. In principle, these problems can all be surmounted by substantial theoretical effort. In the meantime, we conclude that it is difficult to make any definite statements regarding the ionization state of gas close to the burster.

A cloud far from the γ-ray burst will have a low relative velocity corresponding to ordinary galactic rotation. Such a cloud would be an obvious candidate for creating the high-excitation low-velocity absorption component. Another obvious candidate to contribute to the high-excitation low-velocity lines is the shell piled up by the O main-sequence star wind as it blows a bubble in the local ISM at a distance of perhaps 30 pc. Thus, there are two adequate sources of material along the line of sight with distances from 30 to 2500 pc that can be ionized by the burst flux.

3.3. *Accelerating the Gas*

Gas near the burster will receive a tremendous blast of photons, and interactions will transfer some of the photons' momentum to the gas. The total radiative acceleration of the gas that determines its final velocity will occur during the few seconds when the burst flux passes through the gas a few hours before the time at which the absorption lines are produced by the gas. How much momentum gets transferred depends on the cross section of the gas, the spectrum of the burst, and the flux of the burst photons. The final velocity will fall off as the inverse square of the distance from the burst. At some distance, the blast will accelerate the gas to 3000 km s^{-1}, and this process could account for the observed high relative velocity of one of the absorption components. In this subsection, we present a detailed calculation of the radiation-induced velocity as a function of distance from the burster.

The radiative acceleration g_r (as a function of distance R and time t) by a central energy source is given by

$$g_r(R,\ t) = 4\pi c^{-1} \int \sigma(E) m_n^{-1} H_{\rm E}(R,\ t)\, dE\ , \qquad (1)$$

where $\sigma(E)$ is the cross section for interaction with a burst photon of energy E, m_n is the mass per nucleon, and $H_{\rm E}$ is the Eddington flux, which is the first moment of the intensity (with units of ergs cm^{-2} s^{-1} ergs^{-1}). The velocity due to radiative acceleration is

$$v = v_0 + \int_{\Delta t} g_r\, dt\ , \qquad (2)$$

where v_0 is the initial velocity of the gas, and Δt is the time interval covering the burst duration as the photons pass through the gas being accelerated. This integral over time will change the burst flux into a fluence, which is to say that the acceleration only depends on the number of incident photons and not on their time distribution. This change in velocity structure in the gas around the burst will not lead to any significant changes in the density structure on timescales for which we are concerned. That is, a parcel of gas accelerated to, say, 3000 km s^{-1} will move only 1.7 AU in 1 day, so as to cause a $\sim$0.03% density change within a gas clump of size, for example, 10^{17} cm if the backside suffers zero acceleration.

The γ-ray cross sections for the photon-matter interaction have been included as detailed in Höflich et al. (1992). Because the photon energies far exceed the binding energies of the electrons in atoms, the interaction of electrons and photons is given by the Klein-Nishina cross section per nucleon. For lower energies, we determine the angle dependent Klein-Nishina cross section by a standard rejection technique and obtain the cross section by formal integration over angle. Bound-free cross sections have been included according to Veigel (1973). The X-ray opacities are dominated by bound-free transitions from inner shell electrons (which are always populated since when an inner shell electron is ejected it is rapidly filled by one of the outer electrons) and are independent of the conditions in the gas cloud. Thus, the bound-free opacity is rather model-independent.

The final velocities are a function of composition and the burst spectrum. For composition, we adopted either a normal solar abundance (Anders & Grevesse 1989), a Wolf-Rayet composition (Woosley, Langer, & Weaver 1993), or a pure gas of ionized hydrogen. For the spectrum, we adopted broken power laws with a low-energy cutoff, as described in the previous subsection. The results for $v_0 = 0$ are displayed in Figure 2. We find that the composition of the gas has little effect. We find that the flux around 1 keV (in the frame of the host galaxy) is very important, due to the large cross sections associated with bound-free interactions. Unfortunately, the flux for energies below 7 keV are not known, and we can only assume plausible spectral shapes, as discussed in the previous section.

Our favorite model of the final velocity as a function of the radial distance from the burster is represented by the thick line in Figure 2. To accelerate gas from rest to 3000 km s^{-1} implies that the gas is at a distance of 0.2 pc. If the gas were already expanding at a velocity of 2500 km s^{-1}, then the radial distance of the gas would be $\sim$0.5 pc. Gas initially at rest at $\sim$0.5 pc would be accelerated to $\sim$500 km s^{-1}, corresponding to one of the observed absorption components.

If the cloud has a substantial extent along the line of sight, then the inner edge will be accelerated to a higher velocity than the outer edge. This would result in a broad line, instead of the narrow lines observed. The radiative acceleration mechanism thus requires that the intervening cloud be physically narrow. This could arise from a small cloud (as a clumpy part of a wind) or from a thin shell (presumably created by the progenitor). For quantitative limits, the width of the carbon lines appears to be less than 400 km s^{-1}, for which the dominant absorbing region in the shell must be thinner than 7% of its radius provided the gas is accelerated from rest to around 3000 km s^{-1} by the burst radiation. If

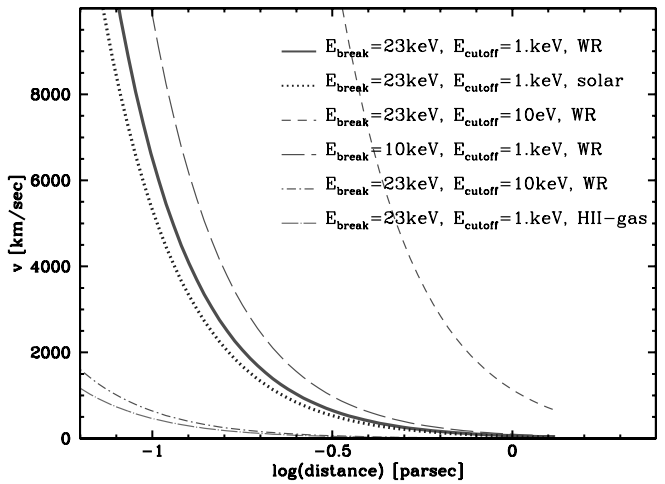

FIG. 2.—Terminal velocity induced by GRB 021004 radiation as a function of distance for three abundances (normal solar abundance, a Wolf-Rayet abundance with little hydrogen and enriched CNO elements, and a pure H II gas) and two values of $E_{\rm break}$ (see text), 10 and 23 keV in the frame of the host galaxy (3 and 7 keV in the Earth frame). The low-energy cutoff in the spectrum, $E_{\rm cutoff}$, (0.01, 1.0, and 10 keV in the host galaxy frame) below which we assume there is zero flux was also varied. The thick solid line represents the case (WR composition, the highest break energy, and flux continuing to 1 keV) that we think is most applicable to GRB 021004. for which gas at a distance of around 0.2 pc could be accelerated from rest to 3000 km s^{-1} by the burst. The derived radial distances depend little on the gas composition. The two lowest curves correspond to cases where the low-energy photons do not interact with the gas by bound-free collisions, demonstrating that most of the acceleration arises from bound-free interactions with low-energy photons. The case with $E_{\rm cutoff} = 0.01$ keV is an extreme situation that we do not think is likely since even a small amount of gas will produce much higher cutoff energies.

the gas already had an initial velocity of 2000 km s^{-1}, then the dominant absorbing region in the shell must be thinner than 21% of its radius. If an absorbing gas has a windlike density distribution (that falls off as the inverse square of the radial distance), then 50% of the absorption will come from between the inner edge of the absorbing region to twice that radius. Thus, for absorption from a smooth wind, the radiative acceleration must be small compared to the initial wind velocity to avoid excessively broad absorption lines. However, if the absorbing gas has a significant clump superposed on a windlike structure (see § 5), then such a clump may be sufficiently thin to form a narrow absorption line despite a large radiative acceleration even in a wind.

This acceleration of gas close to the burster must occur; the only question is the size of the effect. This depends primarily on unknown details of the low-energy photons in the burst spectrum after they have passed through material at small radial distances. For reasonable assumptions ($E_{\rm cutoff} \ll 10$ keV), the radiative acceleration will induce velocity changes of 1000 km s^{-1} or greater for gas within a fraction of a parsec from the burster. This accelerated gas must include that which is creating the afterglow, as well as the dense gas interior to the afterglow shock that represents the inner region of any wind that was driven off the progenitor.

3.4. *Massive Star Winds*

Wolf-Rayet stars are very hot (30,000–70,000 K) stars shedding a thick wind for which the characteristic spectra involve bright and broad emission lines with P Cygni profiles. They are highly evolved stars, the main-sequence masses of which were larger than 35 $M_\odot$ or so. For the most massive stars ($\sim$60 $M_\odot$) the evolutionary path is from an O main-sequence star to a luminous blue variable to a Wolf-Rayet star of the WN class to a Wolf-Rayet star of the WC class to a supernova collapse, while a less massive star ($\sim$35 $M_\odot$) progresses from an O main-sequence star to a red supergiant to a Wolf-Rayet star of the WN class to a supernova collapse. Significant evidence and theoretical models support the hypothesis that long-duration γ-ray bursts are caused by the collapse of massive stars (Wheeler et al. 2000; Woosley & Heger 2001), consistent with the notion that the immediate progenitors of bursts are Wolf-Rayet stars.

Each stage in the evolution of massive stars has a distinct wind (García-Segura, Langer, & Mac Low 1996a; García-Segura, Mac Low, & Langer 1996b). The O main-sequence star wind is characterized by a velocity of $\sim$3000 km s^{-1} and a mass-loss rate on the order of 10^{-6} to 10^{-5} $M_\odot$ yr^{-1}, which lasts for a few million years. The luminous blue variable phase has a massive ejection (at a rate of up to 10^{-3} $M_\odot$ yr^{-1}) over a short time (roughly 10,000 yr) with moderate velocities (around 300 km s^{-1}). The red supergiant wind is characterized by a velocity of 10–100 km s^{-1} and a mass-loss rate of up to 10^{-4} $M_\odot$ yr^{-1}, which lasts for around 200,000 yr. The Wolf-Rayet wind is characterized by velocities of 1000–3000 km s^{-1} and a mass loss from 10^{-5} to 10^{-4} $M_\odot$ yr^{-1} over a lifetime of fractions of a million years.

The interactions between the winds in each successive stage of evolution will create shells with various properties (García-Segura et al. 1996a, 1996b). The O main-sequence star will blow a bubble into the surrounding ISM that has a thin shell and a slow expansion velocity at a distance on the order of 30 pc. The massive ejection of a luminous blue variable will produce a thick shell that expands with a velocity of around 300 km s^{-1}. The red supergiant wind will bunch up at its outer edge and expand with a velocity of 10–100 km s^{-1}. The Wolf-Rayet wind blows a bubble in the slower and denser wind around it, creating a thin shell that expands with a velocity on the order of 500 km s^{-1}. This bubble will overtake the slower shell in $\sim$10,000 yr and coalesce to form a combined turbulent shell. At the time of the core collapse of the star, the inner several parsecs will consist of the Wolf-Rayet wind expanding at 1000–3000 km s^{-1}, surrounded by a dense and turbulent shell expanding at perhaps 500 km s^{-1} at a distance of around 10 pc, surrounded by a relatively low density region evacuated by the O main-sequence star wind, all inside a geometrically thin bubble of material piled up from the ISM. The winds of Wolf-Rayet stars are likely to be anisotropic, and the absorption lines in GRB 021004 were created by only a small geometrical cross section, presumably along the rotation axis of the progenitor star.

Can this wind structure around a very massive star account for the observed velocity components in the absorption lines of GRB 021004? The blueshifted 3000 km s^{-1} component would arise from the dense inner wind driven during the Wolf-Rayet phase. The O main-sequence star wind also has a velocity of 3000 km s^{-1}, but its density has been greatly reduced by its expansion into space so that it should produce only negligible absorption. The requisite density in this radius range could also be provided, in principle, by the slower wind of a lower mass star with lower mass-loss rate; this case would subsequently require more radiative acceleration. If the density in the wind falls off as the inverse square of the radial distance from the star, the

absorption from the wind will be dominated by its inner region, say, 0.2–0.4 pc. This means that the absorption lines would primarily sample a Wolf-Rayet wind emitted over a brief time interval somewhat before the core collapse. Over its lifetime, a Wolf-Rayet wind is roughly constant in velocity, while the wind velocity across the 0.2–0.4 pc region should be even more precisely constant. This could produce a narrow absorption line just as is observed. The blueshifted 560 km s^{-1} absorption component in GRB 021004 could arise from the dense shell created at the outer edge of a Wolf-Rayet wind. This shell is expected to be composed of geometrically thin structures that form a turbulent front width that is roughly a tenth of its radius, which expands at roughly 500 km s^{-1} (García-Segura et al. 1996a, 1996b). The velocity structure within the shell is chaotic and will lead to some broadening of the resultant absorption lines. Thus, expected Wolf-Rayet wind structures can produce the observed 3000 and 560 km s^{-1} components.

What are the expected column densities in the Wolf-Rayet winds? For a mass-loss rate of 3×10^{-5} $M_{\odot}$ yr^{-1}, a wind velocity of 3000 km s^{-1}, and an average atomic weight equal to that of helium, a Wolf-Rayet wind will produce a column density of roughly 3×10^{17} atoms cm^{-2}. The total column density of the shell at the outer edge of a Wolf-Rayet wind is uncertain, but it is likely to be roughly the mass ejected (García-Segura et al. 1996a, 1996b) in the red supergiant phase ($\sim$20 $M_{\odot}$) or the luminous blue variable phase ($\sim$10 $M_{\odot}$) spread over a shell of radius 10 pc. For an average atomic mass like that of helium, the total column density will be on the order of 2×10^{17} atoms cm^{-2} or greater. The two shell components thus have comparable column densities, just as the two absorption lines have comparable equivalent widths.

Are these column densities enough to produce significant absorption lines? For the oscillator strengths of C IV and an assumed velocity dispersion on the order of 100 km s^{-1}, a column density of $\sim 10^{14}$ cm^{-2} for C IV atoms in their ground state will produce an absorption line with an optical depth of unity. With the total column density for a component of a Wolf-Rayet wind at around 3×10^{17} atoms cm^{-2}, the carbon line would produce a significant feature provided that C IV in the ground state is more than $\sim$0.0003 of the nucleons in the wind. A large fraction of the ejecta from Wolf-Rayet stars will be carbon. The various ionization states will all spend almost all the time at their ground level because the decay times are on the order of 10^{-8} s. The question of calculating the fraction of carbon that is ionized to any particular degree (by the radiation from the burst and from the progenitor) is a difficult problem for both the physics and for the lack of knowing the conditions of the gas (§ 3.2). Nevertheless, it is plausible that some significant fraction of the carbon will be 3 times ionized. For one-tenth of the carbon being 3 times ionized, the total column of atoms capable of producing the C IV line in the Wolf-Rayet wind will be $\sim 10^{16}$ atoms cm^{-2}. For such a case, the line will be highly saturated. This estimate has many uncertainties, but it is clear that Wolf-Rayet winds can have sufficient carbon to create the observed absorption lines.

Wolf-Rayet stars often show P Cygni line profiles, with the emission component arising from portions of the shell off the line of sight. If the wind structure described above exists around GRB 021004, we do not expect to see P Cygni profiles. There are two reasons for this. The first is that the γ-ray burst radiation is strongly beamed by the jet, so most of the shell off the line of sight is not illuminated. The second reason is that a flash of illumination on the shell will produce emission lines that are delayed by an amount that varies with position in the shell. For typical shell sizes, the emission component would be spread out over many years and will become too faint to be observable. Thus, the lack of P Cygni profiles in the high-excitation lines of GRB 021004 is not an argument against their origin in a Wolf-Rayet wind.

What is the lower limit on the mass of the original star such that it can still produce the required dense wind? O-type stars with masses of $\sim$30 $M_{\odot}$ can produce dense winds with surrounding shell structures (Kudritzki & Puls 2000) and hence might account for the observed lines in GRB 021004. These stars can have wind velocities up to 3000 km s^{-1} but with mass-loss rates that might be smaller than allowed by our analysis of the spectral energy distribution (see § 4). The evolution of such stars would be from an O main-sequence star to a red supergiant to a blue supergiant with a core collapse at some point. While such a progenitor cannot be called a Wolf-Rayet star, it is still a massive star surrounded by shells and hence could be the progenitor of GRB 021004. Since the clumpy density profile is so uncertain, the only rigorous lower limit we can place on this process is that for core collapse itself, that is, $\sim$8 $M_{\odot}$. For instance, a star that blew up as a red giant might have a carbon-rich wind and hence have the necessary density to give the column depth of C IV. Such a structure would have to rely on radiatively accelerated clumps of matter at $\sim$0.5 pc to produce the lower velocity C IV features in the absence of a shell generated by the blue/red wind boundary.

3.5. *The Progenitor is a Massive Star*

We now have two scenarios that can explain the velocity and ionization structure of the high-excitation absorption lines seen in GRB 021004. The first scenario postulates two gas shells or clumps initially nearly at rest at distances of $\sim$0.2 and $\sim$0.5 pc that are radiatively accelerated to velocities of 3000 and 560 km s^{-1}, respectively, as well as ionized by the flash from the burst itself. The second scenario proposes that the progenitor is a Wolf-Rayet–like star with a wind velocity of 3000 km s^{-1} that is surrounded by a shell with velocity 560 km s^{-1}, the gas of which is ionized by the flux from the progenitor. These two scenarios are actually part of a continuum of similar scenarios where the ionizations and velocities vary from being caused entirely by the progenitor to being caused entirely by the burst. For example, in the second scenario, the original wind might have started at a lower ionization state at a velocity of 1500 km s^{-1} and been accelerated and ionized to the final values by the burst. In all these related scenarios, the absorption lines with near zero velocity are caused by chance clouds along the line of sight as far as 2500 pc from the burster that have been ionized in part by the burst radiation.

In the first scenario, we have to ask why a γ-ray burst progenitor would have two geometrically thin gas clouds at distances of $\sim$0.2 and $\sim$0.5 pc? This is improbable unless there is some causal connection between the clouds and the burster. The presence of two geometrically thin clouds along the line of sight could be caused by two shells around the progenitor or by some number of clumps of gas around the progenitor. In the second scenario, we also have shells of gas centered on the progenitor.

We conclude that the progenitor had shells or clumps of gas centered on it and associated with it. Models where the γ-ray burst arises from the collision of two compact objects in close orbit are substantially less likely because these have no ready supply of gas close to the system. The presence of shells is an unusual situation for stars, as few have multiple shells, although clumps are more likely. The only stellar objects with multiple shells that have any realistic hope of being associated with γ-ray bursts are supernovae and massive stars. Any shell from a supernova would have to be preexisting (as in the supranova model of Vietri & Stella 1998) since the afterglow jet would be far outside any normal supernova ejecta if the supernova and burst exploded simultaneously. Salamanca et al. (2002) point out there are difficulties with producing narrow lines with the observed equivalent width from an old supernova remnant. The narrowness of the absorption lines would require that the ejecta has already cooled and condensed into filaments. The question is then the likelihood of getting multiple filaments of greatly different velocity on our line of sight and the column density of any such filaments.

Ideally, the absorption lines from the $z \cong 2.293$ system can tell us about the abundances of carbon, silicon, hydrogen, and nitrogen in the innermost shell ejected by the progenitor; this can then tell us about the progenitor itself. For example, if the composition is that of a Wolf-Rayet shell of a particular type (perhaps with some swept-up ISM material), then we would even get a good idea of the mass of the progenitor. Unfortunately for this program, we have few lines from the $z \cong 2.293$ system (see the many lines for GRB 010222; Mirabal et al. 2002b). Also, the likelihood that our unresolved lines are saturated implies that the measured equivalent widths will be difficult to convert to abundances. Nevertheless, a full analysis based on our data or the data of, for example, Savaglio et al. (2002), might place useful limits on the abundances of the shell and its possible origin.

An example of such an analysis can be made with respect to the carbon-to-nitrogen abundance. Both atoms have similar ionization potentials and should have somewhat similar ionization fractions into either C IV or N V, the oscillator strengths of the two resonance lines are similar, and the cosmic abundance of nitrogen is down from that of carbon by a factor of 3. So simplistically, we would expect the C IV line to have an equivalent width that is roughly 3 times deeper than that of N V, whereas (see Table 1) we do not see any nitrogen lines and the limit on the equivalent widths is a factor of 4.6. With the likelihood that the C IV line has a saturated core, the implication is that nitrogen is significantly underabundant compared to carbon. This would appear to rule out WN-type Wolf-Rayet stars. The lower mass Wolf-Rayet stars undergo core collapse while the wind is still nitrogen-rich (García-Segura et al. 1996a), whereas the higher mass Wolf-Rayet stars have core collapse after the Wolf-Rayet has turned from a WN to a WC type (García-Segura et al. 1996b). Thus, the lack of a N V line in the spectrum of GRB 021004 appears to imply that the burst progenitor must be among the more massive of Wolf-Rayet stars. Alternatively, the progenitor might be a star for which the original mass was too low ($<30\ M_{\odot}$) to allow it to become a WN-type star, yet it would still have fast and dense winds that are not nitrogen-rich.

The lack of molecular hydrogen absorption can be used to place further limits on the density of the gas near the burster. In the model of Draine & Hao (2002), the column density of excited H_2, $N(H_2^*)$, arises from an ionization/dissociation front the dynamics of which imply that there are natural values of the column depth. For example, an increase in the burst fluence would produce a similar front (only deeper into the molecular cloud) with a similar $N(H_2^*)$, while an increase in the molecular density would produce a front with a narrower width yet with a similar $N(H_2^*)$. The only way to produce a smaller column density is to have UV fluxes that are not sufficient to establish a proper ionization/dissociation front in the molecular hydrogen. This could arise if the molecular cloud were at a great distance (say, 1 kpc) from the burster or if the burster were near the edge of the molecular cloud. Draine calculates that a typical burst will destroy molecular hydrogen in gas with a hydrogen column density of 5×10^{22} cm^{-2} (corresponding to $A_V = 20$ or so). For densities from 100 to 10,000 cm^{-3}, the burst will destroy the molecular hydrogen that could serve as an absorber if it is within roughly 2–200 pc of the edge of the cloud. For the general case of the burst erupting well inside a molecular cloud, the $N(H_2^*)$ will be the value used to calculate the template (see § 2), and this is rejected by our spectrum. We conclude that the lack of molecular hydrogen absorption lines in our spectra indicate that the γ-ray burst is not inside a molecular hydrogen cloud unless it is within $\sim$2–200 pc from its edge.

4. THE SPECTRAL ENERGY DISTRIBUTION

We have constructed broadband fluxes from the radio to the X-ray for several epochs (see Fig. 3) with the data collected from the GCN notices. The major features of the

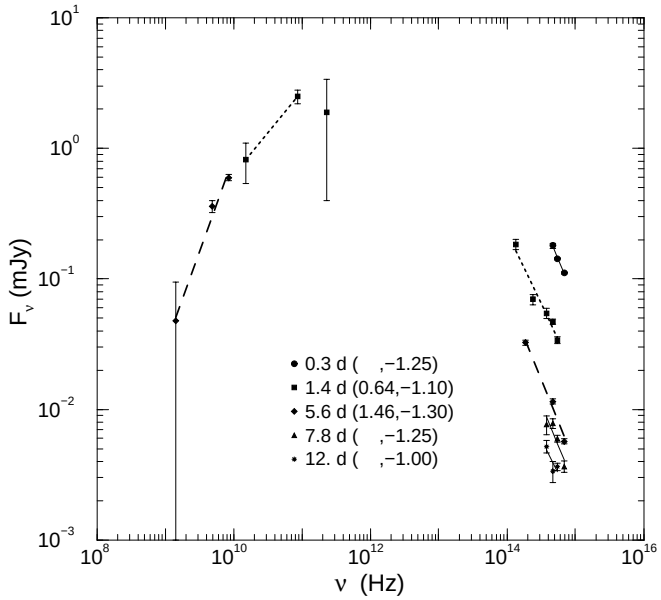

FIG. 3.—Broadband spectrum of GRB 021004 at several epochs. These composite spectra were constructed from measures given in the GCN notices (Balman et al. 2002; Sahu et al. 2002; Pooley 2002; Bremer & Castro-Tirado 2002; Barsukova et al. 2002a; Berger et al. 2002; Di Paola et al. 2002; Stefanon et al. 2002; Malesani et al. 2002b; Williams, Lindsay, & Milne 2002). The optical light is not corrected for extinction in our Milky Way Galaxy (which should be moderately low due to the burst's relatively high galactic latitude). In the plot legend, each line indicates the type of symbol, the epoch for which the observations were obtained in days, while in parentheses the spectral slopes for radio and optical are given. For three epochs, no radio data is available, so the radio spectral slope is left blank.

radio emission are (1) at 0.5–3.5 days the 15 GHz light curve rises as $t^{0.4\pm0.3}$, (2) at 1.5 days the 15–86 GHz spectrum is $F_\nu \propto \nu^{0.6\pm0.2}$, appearing flat from 86 to 230 GHz, and (3) at 5.7 days the 1.4–8.5 GHz spectrum is $F_\nu \propto \nu^{1.0\pm1.6}$. The last two features indicate that the synchrotron self-absorption frequency ν_a is not significantly above 15 GHz at 1.5 days and not much below 8 GHz at 5.7 days, which would suggest a windlike medium (for which $\nu_a \propto t^{-3/5}$) instead of a homogeneous environment (for which ν_a is constant). However, with only a few measurements and the possibility of significant interstellar scintillation affecting the lower frequency (under 15 GHz) observations, it is premature to favor a windlike medium based on the apparent decrease of ν_a over a factor of 4 in time. The rise of the 15 GHz emission is consistent with both the expectations from a homogeneous medium (where $F_\nu \propto t^{1/2}$ irrespective of the location of ν_a) and a behavior intermediate to the asymptotic $F_{\nu \ll \nu_a} \propto t$ and $F_{\nu \gg \nu_a} = \text{const}$ expected for a windlike medium.

Within the framework of relativistic fireballs, consistency between the decay rate of the optical emission ($F_\nu \propto t^{-\alpha_O}$ with $\alpha_O \simeq 1.0$) and spectral slope ($F_\nu \propto \nu^{-\beta_O}$ with $\beta_O \simeq 1.0$) requires that the cooling frequency ν_c is below or within the optical range, as in this case the expected relationship [$\beta_O = (2\alpha_O + 1)/3$, irrespective of the type of external medium] is satisfied. Furthermore, that ν_c is below optical is also consistent with the equality of the optical and X-ray decay indices ($\alpha_X = 1.0 \pm 0.2$; Sako & Harrison 2002) and spectral slopes ($\beta_X = 1.1 \pm 0.1$). We note, however, that the difference between the observed optical and X-ray decay indices, $\alpha_X - \alpha_O = 0.2$, is also consistent (even if only marginally) with the theoretically expected value $\alpha_X - \alpha_O = 0.25$ in the case where ν_c is above the optical domain but below X-rays, and that the intrinsic optical spectral slope β_o can be smaller than observed if there is a significant dust reddening within the host galaxy. Therefore, the cooling frequency could be above the optical domain, in which case one expects that $\beta_o = 2\alpha_O/3 = 2/3$ for a homogeneous medium, and $\beta_o = (2\alpha_O - 1)/3 = 1/3$ for a windlike medium. Furthermore, it is also expected that $\beta_o = \beta_X - 0.5 = 0.6 \pm 0.1$, which favors a homogeneous medium when compared with the above β_o inferred from the optical decay.

Concluding, the currently available radio and optical data for GRB 021004 do not sufficiently constrain the type of external medium, homogeneous or windlike. However, the average density of the medium or the mass-loss rate–to–wind speed ratio can be determined if the cooling frequency lies within the optical range at about 2 days, as suggested by Matheson et al. (2003). Together with the optical measurements, the 15, 86, and 230 GHz fluxes reported by Pooley (2002) and Bremer & Castro-Tirado (2002) indicate that at 1.5 days, the peak of the spectrum of GRB 021004 is $\sim$3 mJy, at a frequency between 10^{11} and 10^{12} Hz. Adding that $\nu_a \simeq 10$ GHz at a few days, these four constraints on the synchrotron spectrum are sufficient to determine the external medium density, fireball isotropic-equivalent energy, and fractional energies in electrons and magnetic fields. We obtain an external density in the range $10^{0.5}$–$10^{2.5}$ cm^{-3} for a homogeneous medium, consistent with the values found by Panaitescu & Kumar (2002) for other GRB afterglows. For a windlike medium, we find that density of the wind corresponds to that resulting from a mass-loss rate–to–wind speed ratio in the range 1 to several times 10^{-5} ($M_\odot$ yr^{-1})/(1000 km s^{-1}), within the range expected for WR stars.

5. THE LIGHT CURVE

We have constructed light curves and color curves for GRB 021004 from data published in the GCN notices (see Fig. 4). Overall, the light curve behaves approximately as a t^{-1} power law, which is normal for many afterglows. However, there are many significant bumps and wiggles about any simple single power law. To help visualize these bumps, the middle panel of Figure 4 shows the R-band light curve after a t^{-1} power law has been subtracted, and we see three bumps with peaks at 0.14, 1.1, and 4.0 days after the burst. The $V-R$ color is plotted in the lower panel of Figure 4. The color appears to remain essentially constant from 0.2 to 10 days.

Afterglow models suggest that light curves should consist of broken power laws, so there is an urge to try to interpret

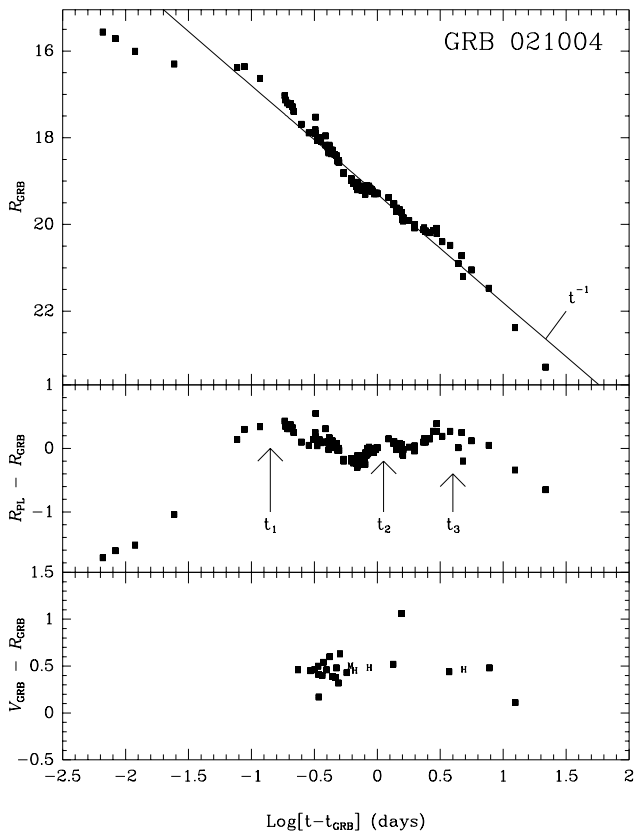

FIG. 4.—Light and color curves for GRB 021004. The top panel displays all R-band magnitudes reported to date in the GCN notices (Fox et al. 2002a; Uemura et al. 2002; Oksanen et al. 2002a, 2002b; Weidinger et al. 2002; Winn et al. 2002; Zharikov et al. 2002; Halpern et al. 2002a, 2002b; Balman et al. 2002; Cool et al. 2002; Bersier et al. 2002; Sahu et al. 2002; Matsumoto et al. 2002; Covino et al. 2002a, 2002b; Holland et al. 2002b; Stanek et al. 2002; Mirabal et al. 2002a, 2002c; Masetti et al. 2002; Barsukova et al. 2002a, 2002b; Malesani et al. 2002a, 2002b; Klotz et al. 2002a, 2002b; Di Paola et al. 2002; Stefanon et al. 2002; Lindsay et al. 2002a, 2002b; Williams et al. 2002; Garnavich & Quinn 2002). The magnitudes have all been reduced to the system reported by Henden (2002). For comparison, a t^{-1} power law is shown. The middle panel shows the same data with the t^{-1} power law subtracted. The important point is that the brightness displays three peaks or bumps, centered at times of roughly 0.14, 1.1, and 4.0 days after the burst. The bottom panel shows the $V-R$ color. Most of the V magnitudes reported in the GCN are from one single interval (0.3–0.6 days after the burst). Our $V-R$ colors from synthetic photometry of the HET and McDonald 2.7 m spectra are marked as "H" and "M," respectively. We see that the $V-R$ color does not change significantly over the interval from 0.2 to 10 days.

Figure 4 in terms of broken power laws. Perhaps the basic behavior is t^{-1} with bumps and some separate mechanism for the dimness at the earliest times. Alternatively, perhaps the basic behavior is a $t^{-0.7}$ power law up until a break at 3 days to a $t^{-1.5}$ power law with a particularly strong bump from 0.1 to 0.7 days. For a third alternative, perhaps the basic behavior is a $t^{-1.5}$ decline over the entire time range except that some mechanism inserts more energy three times during the decline (at 0.14, 1.1, and 4.0 days).

In general, γ-ray burst afterglows have simple power-law declines in brightness, often with a break ascribed to collimation of the outflow. Nevertheless, many γ-ray bursts have bumps in their afterglows. For example, the optical brightness of the afterglow of GRB 970508 increased by 1.5 mag 1–2 days after the γ-ray burst (Garcia et al. 1998). GRB 970508 was seen by the *BeppoSAX* satellite to have a significant brightening in its X-ray light curve starting at 16 hr after the burst (Piro et al. 1999). GRB 000301c displayed an achromatic bump that peaked around 4 days after the burst that has been ascribed to gravitational microlensing by Garnavich, Loeb, & Stanek (2000). In addition, three γ-ray bursts with bumps around 30 days after the burst have been ascribed to an underlying supernova (Reichart 1999; Bloom et al. 1999, 2002; but see Dermer 2002) or dust echos (Reichart 2001).

The presence of bumps in otherwise-smooth afterglow light curves has previously been attributed to microlensing, dust echos, and supernovae. Now we have a burst with three bumps, and they cannot all be due to microlensing, dust echos, or supernovae, so we have proof that afterglows can makes bumps on various timescales for other reasons. Thus, the mere presence of a single bump can only provide poor support for any particular proposed cause unless other possibilities can be excluded by some means. For example, the red color of a bump (compared to the underlying afterglow) cannot be taken as substantial evidence of a supernova origin until the cause and color-distribution of other classes of bumps are known.

There are two generic scenarios (in addition to microlensing, dust echos, and supernovae) for producing variability in the afterglow emission: an inhomogeneous circumburst medium and nonuniform properties of the γ-ray burst ejecta (see also Nakar, Piran, & Granot 2003). Inhomogeneities in the external gas could be either in the form of clumps of denser material (Wang & Loeb 2000), which enhance the dissipation of the kinetic energy of the γ-ray burst remnant and, implicitly, the afterglow brightness, or in the form of a stratified medium, consisting of shells of various densities (Lazzati et al. 2002), perhaps produced by fluctuations in the wind blown by the γ-ray burst progenitor not long before the release of the γ-ray burst ejecta. Nonuniformities in the γ-ray burst ejecta could be manifest as either a range of initial Lorentz factors within an impulsive ejection or as a nonisotropic distribution of the ejecta energy per solid angle. In the former case, the slower part of the outflow catches up with the faster part as the latter is decelerated, enhancing the afterglow kinetic energy and, hence, its brightness. In the latter case, the regions of higher angular energy density are bright spots on the ejecta surface, moving slightly off the direction toward the observer, so that fluctuations in the afterglow emission are produced as the spots decelerate and the widening cone of their relativistically beamed emission starts to include the direction toward the observer. The variable Lorentz factor and anisotropic outflow scenarios have been used to explain the brightening of the afterglow of GRB 970508 by Panaitescu, Mészáros, & Rees (1998) and Panaitescu & Kumar (2002), respectively.

An energy input that is extended in time prior to the brightening at 0.14 days could explain the shallower decline prior to 0.14 days, while an inhomogeneous shell with a density decreasing with radius (Lazzati et al. 2002) could account for the steeper light-curve decay after 0.1 days in the stratified medium scenario. The faster decline after a brightening is consistent with the expectations from scenarios involving dense clumps or bright spots, where the contribution of the clump or spot to the total afterglow emission decreases in time as the fireball decelerates, and more of the uniform ejecta surface becomes visible for the observer.

In the latter two scenarios where the afterglow emission from clumps or spots declines with time, the afterglow light curve should eventually recover its initial decay rate. In this context, the observed light curve is consistent with the proposal that the $t^{-0.7}$ falloff seen in the first 15 minutes reappeared at 0.7 days, just about the time the spectra reported here were obtained, and lasted until 1–3 days after the burst, when the light curve steepened to $t^{-1.0}$. If this interpretation is correct, GRB 021004 would display the shallowest light-curve break ever observed. The change in the break index would be $\simeq 0.3$, suggesting that the break is caused by the passage of the cooling break through the optical domain (Panaitescu & Kumar 2001). The existence of a break in the optical spectrum at 1–3 days is supported by the spectroscopic observations by Matheson et al. (2003) and this paper (see § 2), that the blue part of the optical spectrum reddens between less than 1 and greater than 2.8 days. This interpretation is consistent with a break frequency that decreases in time, implying that the external medium is homogeneous rather than windlike. In the case of a wind, the cooling frequency should increase at least as fast as $t^{1/2}$ (Panaitescu & Kumar 2001). We note, however, that the break in the optical spectrum seems too sharp in wavelength to be due to the cooling break (across which the slope of the power-law spectrum changes by 0.5) and that the spectral changes may not sufficiently affect the *R*-band light curve at a few days to explain the *R*-band light-curve behavior.

The radial distance of the jet from the center of the progenitor as a function of the observer's time should be correlated with the location of clumps and the epoch of the light-curve bumps. This can be modeled given both the broadband spectrum and the light curve by the methods presented in Panaitescu & Kumar (2001, 2002). Unfortunately, only preliminary input numbers are available (for example, no jet break has yet been definitely timed), and details of the external medium are not known (for example, whether or not the average density falls off like a wind). Nevertheless, it is possible to give estimates that are useful for producing a reasonable picture. For this, we adopt the isotropic equivalent energy of the fireball equal to 5.6×10^{52} ergs (Malesani et al. 2002a). If the jet is expanding into an external medium with a windlike structure, then we find that the mass-loss rate to wind-speed ratio is roughly $2 \times 10^{-5}\ M_{\odot}$ per 1000 km s^{-1} (see § 4). In this case, the radius of the jet will be $t^{0.5} \times 0.06$ pc, with t measured in days. If the jet is expanding into a homogenous medium of constant density, then we find that the density is roughly 30 cm^{-3} (see § 4). In this case, the radius of the jet will be $t^{0.25} \times 0.07$ pc.

If the light-curve bumps are due to density enhancements in the surrounding medium, then we can estimate the

approximate radial distances from the burst and overdensities for each clump. For peaks in the light curve at 0.14, 1.1, and 4.0 days, we find approximate radii for the density clumps of 0.022, 0.063, and 0.12 pc, respectively, for a windlike medium. We get similar results for expansion into a homogenous medium with parameters as derived above. The excess light in the light-curve bumps will scale roughly as the square root of the overdensity compared to the "background" density, for the case where the clump is relatively large compared to the visible region (as for a shell). From Figure 4, the extra light in each of the bumps is roughly 0.6, 0.3, and perhaps 0.3 mag; this corresponds to overdensities of roughly 50%, 10%, and 10%. If the bumps are due to clumps, the broadband spectral slopes should remain the same, and thus the colors would not change across the bump, as observed.

At some time the afterglow jet will collide with the gas that is causing the $z \cong 2.293$ absorption. When this happens, we would expect that the afterglow will brighten significantly if the gas is in a relatively narrow shell. We also expect that the associated absorption lines would disappear. We note that our late HET spectrum still showed the $z \cong 2.293$ C IV line with moderately low significance at a time of 4.84 days after the burst when the jet would have reached $\sim$0.13 pc. In principle, we can predict the date at which this bump in the afterglow decline should occur. In practice, such a prediction has substantial uncertainties, primarily in the exact radius of the shell and the density structure of the medium inside the shell. In the case where a shell of material has been radiatively accelerated to 3000 km s^{-1}, the shell will have a radius not much larger than 0.1 pc, and it should be overrun sometime between roughly 2 and 40 days after the burst. In the case where the absorption is due to a Wolf-Rayet wind that extends out to several parsecs, the 3000 km s^{-1} component will be completely eliminated only after many years. The absorption will slowly diminish during the first few months after the burst as the jet catches up with the densest inner part of the wind. In summary, the absorbing gas might be eliminated during the early days after the burst (an event that could be directly observable) or it might take many years to be eliminated (and be totally unobservable).

6. CONCLUSIONS

The GRB 021004 spectrum displays high-ionization and high-velocity absorption lines. We argue that these lines are likely to have arisen from shells of gas around the progenitor star, and further, that these shells plausibly come from a progenitor that was descended from a massive star. The gas in these shells was partially ionized and accelerated by the photons from the burst.

We have used the optical spectrum, the broadband spectrum, and the light curve to identify six components in the medium external to the γ-ray burst. The $z \cong 2.293$ absorption lines arise from a shell at a radial distance of less than a parsec that is moving at a velocity of 3000 km s^{-1} after being ionized and accelerated by the burst radiation. We identify this component as being the wind from the progenitor star, perhaps a Wolf-Rayet star with a mass-loss rate of $\sim 6 \times 10^{-5}\ M_{\odot}$ yr^{-1} or a lower mass star wind accelerated by the bust. This same component provides the external medium with which the jet is colliding to produce the afterglow light. This inner component is probably significantly clumped in order to prevent complete ionization and to facilitate recombination, thus allowing a significant column depth of C IV. The second component is associated with the absorption lines moving 560 km s^{-1} with respect to the host galaxy velocity. We identify this component as arising from a shell of material plowed up by the Wolf-Rayet–like wind at a radius on the order of 10 pc. Alternatively, this feature could be a shell or clump at $\sim$0.5 pc accelerated by the burst. The third component gives rise to the low-velocity high-excitation absorption lines that must come from a distance between tens and hundreds of parsecs from the burster. This component might be from the shell created by the O main-sequence star wind, or it might be from chance ISM clouds along the line of sight, perhaps part of the same star-forming region that gave birth to the γ-ray burst progenitor. The fourth, fifth, and sixth components are three density enhancements that occur in the Wolf-Rayet–like wind at radial distances of 0.022, 0.063, and 0.12 pc so as to produce the three bumps in the light curve. These clumps could be related to the clumping we deduce for component 1, that is, all could be associated with knots in the progenitor wind.

The results summarized in the previous paragraph offer a plausible description of the density structure near this burst. What we see is a variety of density enhancements along the line of sight, with the evidence coming from bumps in the light-curve decline and absorption lines in the spectrum. This picture is apparently not universal for γ-ray bursts, since only two out of nine bursts with well-observed afterglow spectra show both high-excitation and high-velocity lines. The other bursts must have some mechanism for suppressing similar absorption lines.

A full analysis is needed for the $z \sim 2.3$ lines of GRB 021004, with the possibility of determining the abundance of the progenitor's shell and hence to obtain information about the progenitor itself. As a start to this program, we have shown that the nitrogen in the shell is underabundant with respect to the carbon, and this demonstrates that the progenitor was not a WN-type Wolf-Rayet star and further that the progenitor was either one of the more massive Wolf-Rayet stars or a massive star that is below that required to make a WN-type star. A further program for our community is to obtain high-dispersion spectroscopy so as to be able to measure fine velocity structures and faint lines in the afterglow spectra of many bursts.

The most important result from our data and analysis is that a plausible way to create the high-excitation and high-velocity absorption lines is to have shells of gas surrounding the progenitor, and that a realistic way to achieve this is for the progenitor to be a star descended from a massive O-type main-sequence star. This strongly suggested connection to a massive star is much more direct than the moderate statistical association of γ-ray bursts with parts of galaxies undergoing star formation and is much more convincing than attributing poorly observed bumps in afterglow light curves to some associated supernova event. As such, we believe that the absorption lines in the GRB 021004 spectra provide the first strong and direct argument for associating a normal γ-ray burst with a massive progenitor star surrounded by shells.

We thank Bruce Draine, Bev Wills, Greg Shields, and D. J. Hillier for their discussion on a wide range of topics. This work was supported in part by NASA Grant NAG59302 and NSF Grant AST-0098644. The Marcario

Low Resolution Spectrograph is a joint project of the Hobby-Eberly Telescope partnership and the Instituto de Astronomia de la Universidad Nacional Autonoma de Mexico. The Hobby-Eberly Telescope is operated by McDonald Observatory on behalf of the University of Texas at Austin, the Pennsylvania State University, Stanford University, Ludwig-Maximilians-Universität München, and Georg-August-Universität Goettingen.

REFERENCES

Anders, E., & Grevesse, N. 1989, Geochim. Cosmochim. Acta, 53, 197
Balman, S., et al. 2002, GCN Circ. 1580 (http://gcn.gsfc.nasa.gov/gcn/gcn3/1580.gcn3)
Barsukova, E. A., et al. 2002a, GCN Circ. 1606 (http://gcn.gsfc.nasa.gov/gcn/gcn3/1606.gcn3)
———. 2002b, GCN Circ. 1654 (http://gcn.gsfc.nasa.gov/gcn/gcn3/1654.gcn3)
Barth, A. J., et al. 2002, preprint (astro-ph/0212554)
Berger, E., et al. 2002, GCN Circ. 1613 (http://gcn.gsfc.nasa.gov/gcn/gcn3/1613.gcn3)
Bersier, D., Winn, J., Stanek, K. Z., & Garnavich, P. 2002, GCN Circ. 1586 (http://gcn.gsfc.nasa.gov/gcn/gcn3/1586.gcn3)
Bloom, J. S., et al. 1999, Nature, 401, 453
———. 2002, ApJ, 572, L45
Bremer, M., & Castro-Tirado, A. 2002, GCN 1590 (http://gcn.gsfc.nasa.gov/gcn/gcn3/1590.gcn3)
Castander, F. J., et al. 2002, GCN Circ. 1599 (http://gcn.gsfc.nasa.gov/gcn/gcn3/1599.gcn3)
Chornock, R., & Filippenko, A. V. 2002, GCN Circ. 1605 (http://gcn.gsfc.nasa.gov/gcn/gcn3/1605.gcn3)
Cool, R. J., et al. 2002, GCN Circ. 1584 (http://gcn.gsfc.nasa.gov/gcn/gcn3/1584.gcn3)
Covino, S., et al. 2002a, GCN Circ. 1595 (http://gcn.gsfc.nasa.gov/gcn/gcn3/1595.gcn3)
———. 2002b, GCN Circ. 1622 (http://gcn.gsfc.nasa.gov/gcn/gcn3/1622.gcn3)
Dermer, C. D. 2002, preprint (astro-ph/0204037)
Di Paola, A., et al. 2002, GCN Circ. 1616 (http://gcn.gsfc.nasa.gov/gcn/gcn3/1616.gcn3)
Djorgovski, S. G., et al. 2002, GCN Circ. 1620 (http://gcn.gsfc.nasa.gov/gcn/gcn3/1620.gcn3)
Draine, B. T., & Hao, L. 2002, ApJ, 569, 780
Eracleous, M., et al. 2002, GCN Circ. 1579 (http://gcn.gsfc.nasa.gov/gcn/gcn3/1579.gcn3)
Fox, D. W., et al. 2002a, GCN Circ. 1564 (http://gcn.gsfc.nasa.gov/gcn/gcn3/1564.gcn3)
———. 2002b, GCN Circ. 1569 (http://gcn.gsfc.nasa.gov/gcn/gcn3/1569.gcn3)
Frail, D. A., et al. 2001, ApJ, 562, L55
García-Segura, G., Langer, N., & Mac Low, M.-M. 1996a, A&A, 316, 133
García-Segura, G., Mac Low, M.-M., & Langer, N. 1996b, A&A, 305, 229
Garcia, M., et al. 1998, ApJ, 500, L105
Garnavich, P. L., Loeb, A., & Stanek, K. Z. 2000, ApJ, 544, L11
Garnavich, P., & Quinn, J. 2002, GCN Circ. 1661 (http://gcn.gsfc.nasa.gov/gcn/gcn3/1661.gcn3)
Gerardy, C. L., & Fesen, R. A. 2001, AJ, 121, 2781
Halpern, J. P., et al. 2002a, GCN Circ. 1578 (http://gcn.gsfc.nasa.gov/gcn/gcn3/1578.gcn3)
———. 2002b, GCN Circ. 1593 (http://gcn.gsfc.nasa.gov/gcn/gcn3/1593.gcn3)
Henden, A. A. 2002, GCN Circ. 1630 (http://gcn.gsfc.nasa.gov/gcn/gcn3/1630.gcn3)
Hill, G. J., Nicklas, H., MacQueen, P. J., de Tejada, V., C., Cobos, D., F. J., & Mitsch, W. 1998, Proc. SPIE, 3355, 375
Hill, G. J., Wolf, M. J., Tufts, J. R., & Smith, E. C. 2003, Proc. SPIE, in press
Höflich, P., Khokhlov, A., & Müller, M. 1992, A&A, 259, 549
Holland, S. T., et al. 2002a, AJ, 124, 639
———. 2002b, GCN Circ. 1597 (http://gcn.gsfc.nasa.gov/gcn/gcn3/1597.gcn3)
Klotz, A., et al. 2002a, GCN Circ. 1614 (http://gcn.gsfc.nasa.gov/gcn/gcn3/1614.gcn3)
———. 2002b, GCN Circ. 1615 (http://gcn.gsfc.nasa.gov/gcn/gcn3/1615.gcn3)
Kudritzki, R.-P., & Puls, J. 2000, ARA&A, 38, 613
Lamb, D. Q., et al. 2002, GCN Circ. 1600 (http://gcn.gsfc.nasa.gov/gcn/gcn3/1600.gcn3)
Landolt, A. U. 1992, AJ, 104, 340
Lazzati, D., & Perna, R. 2002, MNRAS, 330, L383
Lazzati, D., Rossi, E., Covino, S., Ghisellini, G., & Malesani, D. 2002, A&A, 396, L5
Lindsay, K., Hartmann, D. H., Davis, K., & Leising, M. 2002a, GCN Circ. 1638 (http://gcn.gsfc.nasa.gov/gcn/gcn3/1638.gcn3)
Lindsay, K., Hartmann, D. H., & Tassinari, J. 2002b, GCN Circ. 1628 (http://gcn.gsfc.nasa.gov/gcn/gcn3/1628.gcn3)
Lotz, W. 1967, ApJS, 14, 207
Malesani, D., et al. 2002a, GCN Circ. 1607 (http://gcn.gsfc.nasa.gov/gcn/gcn3/1607.gcn3)
———. 2002b, GCN Circ. 1645 (http://gcn.gsfc.nasa.gov/gcn/gcn3/1645.gcn3)
Masetti, N., et al. 2002, GCN Circ. 1603 (http://gcn.gsfc.nasa.gov/gcn/gcn3/1603.gcn3)
Matheson, T., et al. 2003, ApJ, 582, L5
Matsumoto, K., et al. 2002, GCN Circ. 1594 (http://gcn.gsfc.nasa.gov/gcn/gcn3/1594.gcn3)
Mirabal, N., Halpern, J. P., Chornock, R., & Filippenko, A. V. 2002a, GCN Circ. 1618 (http://gcn.gsfc.nasa.gov/gcn/gcn3/1618.gcn3)
Mirabal, N., et al. 2002b, ApJ, 578, 818
———. 2002c, GCN Circ. 1602 (http://gcn.gsfc.nasa.gov/gcn/gcn3/1602.gcn3)
Møller, P., et al. 2002, A&A, 396, L21
Nakar, E., Piran, T., & Granot, J. 2002, NewA, submitted (astro-ph/0210631)
Oksanen, A., et al. 2002a, GCN Circ. 1570 (http://gcn.gsfc.nasa.gov/gcn/gcn3/1570.gcn3)
———. 2002b, GCN Circ. 1591 (http://gcn.gsfc.nasa.gov/gcn/gcn3/1591.gcn3)
Panaitescu, A., & Kumar, P. 2001, ApJ, 554, 667
———. 2002, ApJ, 571, 779
Panaitescu, A., Mészáros, P., & Rees, M. J. 1998, ApJ, 503, 314
Piro, L., et al. 1999, ApJ, 514, L73
———. 2000, Science, 290, 955
Pooley, G. 2002, GCN Circ. 1588 (http://gcn.gsfc.nasa.gov/gcn/gcn3/1588.gcn3)
Reichart, D. E. 1999, ApJ, 521, L111
———. 2001, ApJ, 554, 643
Sahu, D. K., et al. 2002, GCN Circ. 1587 (http://gcn.gsfc.nasa.gov/gcn/gcn3/1587.gcn3)
Sako, M., & Harrison, F. 2002, GCN Circ. 1624 (http://gcn.gsfc.nasa.gov/gcn/gcn3/1624.gcn3)
Salamanca, I., Rol., E., Wijers, R., Ellison, S., Kaper, L., & Tanvir, N. 2002, GCN Circ. 1611 (http://gcn.gsfc.nasa.gov/gcn/gcn3/1611.gcn3)
Sargent, W. L. W., Steidel, C. C., & Boksenberg, A. 1988, ApJS, 68, 539
Savaglio, S., et al. 2002, GCN Circ. 1633 (http://gcn.gsfc.nasa.gov/gcn/gcn3/1633.gcn3)
Schaefer, B. E. 2003, ApJ, 583, L67
Schaefer, B. E., Deng, M., & Band, D. L. 2001, ApJ, 563, L123
Shiraski, Y., et al. 2002, GCN Circ. 1565 (http://gcn.gsfc.nasa.gov/gcn/gcn3/1565.gcn3)
Stanek, K. Z., Bersier, D., Winn, J., & Garnavich, P. 2002, GCN Circ. 1598 (http://gcn.gsfc.nasa.gov/gcn/gcn3/1598.gcn3)
Stefanon, M., et al. 2002, GCN Circ. 1623 (http://gcn.gsfc.nasa.gov/gcn/gcn3/1623.gcn3)
Uemura, M., et al. 2002, GCN Circ. 1566 (http://gcn.gsfc.nasa.gov/gcn/gcn3/1566.gcn3)
Veigel, W. J. 1973, At. Data Nucl. Data Tables, 5, 51
Vietri, M., & Stella, L. 1998, ApJ, 507, L45
Vreeswijk, P. M., et al. 2001, ApJ, 546, 672
Wang, X., & Loeb, A. 2000, ApJ, 535, 788
Weidinger, M., et al. 2002, GCN Circ. 1573 (http://gcn.gsfc.nasa.gov/gcn/gcn3/1573.gcn3)
Wheeler, J. C., Yi, I., Höflich, P., & Wang, L. 2000, ApJ, 537, 810
Williams, G., Lindsay, K., & Milne, P. 2002, GCN Circ. 1652 (http://gcn.gsfc.nasa.gov/gcn/gcn3/1652.gcn3)
Winn, J., et al. 2002, GCN Circ. 1576 (http://gcn.gsfc.nasa.gov/gcn/gcn3/1576.gcn3)
Woosley, S. E., & Heger, A. 2001, BAAS, 198, 3801
Woosley, S. E., Langer, N., & Weaver, T. A. 1993, ApJ, 411, 823
Zharikov, S., Vazquez, R., Benitez, G., & del Rio, S. 2002, GCN Circ. 1577 (http://gcn.gsfc.nasa.gov/gcn/gcn3/1577.gcn3)